Electronic Supplementary Material (ESI) for Environmental Science: Processes & Impacts.


# Use of Optical Properties for Evaluating the Presence of Pyrogenic Organic Matter in Thermally Altered Soil Leachates

Garrett McKay,[1*] Amanda K. Hohner,[2*] and Fernando L. Rosario-Ortiz[3]

[1]Zachry Department of Civil and Environmental Engineering, Texas A&M University, College Station, TX; [2]Department of Civil and Environmental Engineering, Washington State University, Pullman, WA; [3]Department of Civil, Environmental, and Architectural Engineering, University of Colorado Boulder, Boulder, CO

*Corresponding authors: gmckay@tamu.edu; ahohner@wsu.edu
Submitted to *Environmental Science: Processes and Impacts*

**Electronic Supplemental Information**

## Supplementary Tables

Table S 1. List of samples analyzed in this study including place of origin, type, and heating temperature.

| ***Two Colorado sites, Nederland (NED) and Flagstaff (FLG), heated at 100, 150, 250, 350, 450, and 550 ºC. Mineral and organic layers separated during heating and leaching.*** | | | | |
|---|---|---|---|---|
| Sample Name | Heating Temp. (ºC) | Layer | Coordinates | Characteristics |
| NEDCTRL | CTRL | Organic | 39°58’52”N 105°31’07”W | The NED site had no closed canopy with understory vegetation characterized by blue grama grass (*Bouteloua gracilis)*, needle-and-thread grass (*Hesperostipa comate*), and western wheatgrass (*Pascopyrum smithii*). The NED soil series is moderately permeable and well-drained, characterized by a cobbly sandy loam. |
| NED150 | 150 | | | |
| NED250 | 250 | | | |
| NED350 | 350 | | | |
| NED450 | 450 | | | |
| NEDCTRL | CTRL | Mineral | | |
| NED150 | 150 | | | |
| NED250 | 250 | | | |
| NED350 | 350 | | | |
| NED450 | 450 | | | |
| NED550 | 550 | | | |
| FLGCTRL | CTRL | Organic | 39°59’51”N 105°18’33”W | The FLG site samples were taken under closed canopy, which was characterized by coniferous forest stands comprised of ponderosa pine, Douglas-fir, and subalpine fir-Engelmann spruce (*Picea engelmanni, Abies lasiocarpa*). There was no prominent understory vegetation; however, a layer of fallen litter consisting chiefly of pine needles was present and was removed prior to mineral soil excavation. |
| FLG150 | 150 | | | |
| FLG250 | 250 | | | |
| FLG350 | 350 | | | |
| FLG450 | 450 | | | |
| FLGCTRL | CTRL | Mineral | | |
| FLG150 | 150 | | | |
| FLG250 | 250 | | | |
| FLG350 | 350 | | | |
| FLG450 | 450 | | | |
| FLG550 | 550 | | | |
| ***Colorado (DW, WM) and New York (NY) samples unheated and heated at 225 ºC. Mineral and organic layers combined during heating and leaching.*** | | | | |
| Sample Name | Heating Temp. (ºC) | Layer | Approximate Location | Characteristics |
| DW1 | CTRL | Composite of organic and mineral layers | Gross Reservoir, Boulder Creek Watershed, Boulder County, CO | 2202 m elevation in Roosevelt National forest, northwest of Denver, CO, USA. Granite bedrock drainage, clay content of soils in drainage area is ~ 15%. Watershed is a mountainous, forested area, consisting of ponderosa and lodgepole pines and mixed conifers. |
| DW1225 | 225 | | | |
| DW2 | CTRL | | | |
| DW2225 | 225 | | | |
| DW3 | CTRL | | | |
| DW3225 | 225 | | | |
| NYEA | CTRL | | Ashokan Reservoir, Catskill/Deleware Watersheds | 5180 km$^2$ watershed. Located ~160 km northwest of New York City, west of Hudson River. Sedimentary bedrock of sandstone and shale. Tree species range from northern hardwood trees such as maple and birch, to white pine, elm, and ash. |
| NYEA225 | 225 | | | |
| NYKEN | CTRL | | Kensico Reservoir, Croton Watershed | |
| NYKEN225 | 225 | | | |
| NYNN | CTRL | | Neversink Reservoir, Catskill/Deleware Watersheds | |
| NYNN225 | 225 | | | |
| NYRR | CTRL | | Rondout Reservroir, Catskill/Deleware Watersheds | |
| NYRR225 | 225 | | | |
| WM35 | CTRL | | Clear Creek watershed, Jefferson County, CO. | Similar vegetation to Gross Reservoir. Geology composed of crystalline rocks, including granite and gneiss, with quartz and pyrite minerals. Soil clay content is ~ 12%. |
| WM35225 | 225 | | | |
| WM40 | CTRL | | | |
| WM40225 | 225 | | | |
| WM49 | CTRL | | | |
| WM49225 | 225 | | | |

Table S 2. Optical indices used in this study and their associated calculation methods.

| Absorbance/Fluorescence | Parameter | Calculation method | Comment |
|---|---|---|---|
| Absorbance | *E2/E3* | *E2/E3* = $Abs_{250}/Abs_{365}$ | - |
| | $S_{300\text{-}600}$ (spectral slope, $nm^{-1}$) | $Abs(\lambda) = Abs(350nm) \times \exp(-S_{300\text{-}600}(\lambda\text{-}350nm))$ | Non-linear fitting to calculate $S_{300\text{-}600}$ |
| | $S_R$ (spectral slope ratio) | $S_R = slope_{275\text{-}295} / slope_{350\text{-}400}$ | Slope is obtained from linear regression of log-transformed absorbance versus wavelength values |
| | $SUVA_{254}$ (specific ultraviolet absorbance at 254 nm) | $SUVA_{254} = Abs_{254} / DOC \times 100$ (L $mg_C^{-1}$ $m^{-1}$) | Absorbance values are in decadic system |
| | $UV_{254}$ (ultraviolet absorbance at 254 nm) | - | Absorbance at 254 nm |
| Fluorescence | $\Phi_f$ (fluorescence quantum yield) | $\Phi_{f,DOM} = \Phi_{f,QS} \frac{F_{DOM}}{F_{QS}} \frac{f_{QS}}{f_{DOM}} \frac{n^2_{DOM}(\lambda_{em})}{n^2_{QS}(\lambda_{em})}$ | See main text and ref. [1] |
| | Regional peak intensities (RU) | <u>Regional approach</u>: A(260,426), B(280,310), C(320,440), T(280,338) <u>Algorithm-based approach:</u> A(240-270,380-470), B(260-290, 300-320), C(300-340,400-480), T(260-290,326-350) | <u>Regional approach:</u> Excitation/Emission pairs in nm for peaks A, B, C, T <u>Algorithm-based approach:</u> Excitation/Emission ranges in nm for peaks A, B, C, T |
| | Specific regional peak intensities (RU L $mg_C^{-1}$) | Same as above but divided by DOC | - |
| | FI (Fluorescence index) | FI = $Em_{370}/Em_{420}$ at Ex = 370 nm | See main text regarding appropriateness of FI for these samples |

Table S 3. Selected elemental concentrations in Nederland and Flagstaff mineral soil leachates.

| Sample | **P (mg/L)** | **Si (mg/L)** | **Mn (mg/L)** | **Fe (mg/L)** | **Mg (mg/L)** | **Ca (mg/L)** | **Al (mg/L)** | **Na (mg/L)** | **K (mg/L)** |
|---|---|---|---|---|---|---|---|---|---|
| NEDCTRL | <LOQ | 0.119 ± 0.031 | <LOQ | <LOQ | 0.054 ± 0.002 | 0.199 ± 0.015 | 0.014 ± 0.000 | 0.047 ± 0.011 | 0.712 ± 0.190 |
| NED150 | <LOQ | 0.153 ± 0.027 | 0.006 ± 0.001 | <LOQ | 0.122 ± 0.007 | 0.479 ± 0.022 | 0.015 ± 0.001 | 0.043 ± 0.022 | 0.797 ± 0.148 |
| NED250 | 0.491 ± 0.591 | 0.254 ± 0.022 | 0.151 ± 0.007 | 0.016 ± 0.003 | 0.577 ± 0.014 | 2.923 ± 0.024 | 0.051 ± 0.002 | 0.097 ± 0.082 | 37.542 ± 72.710 |
| NED350 | 0.139 ± 0.002 | 0.242 ± 0.013 | 0.014 ± 0.002 | <LOQ | 0.383 ± 0.024 | 2.886 ± 0.232 | 0.105 ± 0.003 | 0.043 ± 0.015 | 0.958 ± 0.161 |
| NED450 | 0.172 ± 0.055 | 0.276 ± 0.006 | <LOQ | <LOQ | 0.254 ± 0.007 | 2.818 ± 0.058 | 0.454 ± 0.017 | 0.081 ± 0.027 | 0.850 ± 0.106 |
| FLGCTRL | <LOQ | 0.037 ± 0.004 | 0.005 ± 0.001 | <LOQ | 0.037 ± 0.001 | 0.124 ± 0.010 | 0.022 ± 0.002 | 0.034 ± 0.005 | 0.659 ± 0.120 |
| FLG150 | 0.121 ± 0.019 | 0.063 ± 0.013 | 0.038 ± 0.003 | <LOQ | 0.137 ± 0.004 | 0.506 ± 0.012 | 0.042 ± 0.012 | 0.042 ± 0.012 | 1.093 ± 0.156 |
| FLG250 | 0.137 ± 0.019 | 0.085 ± 0.032 | 0.135 ± 0.017 | 0.032 ± 0.008 | 0.291 ± 0.041 | 1.379 ± 0.167 | 0.096 ± 0.015 | 0.061 ± 0.007 | 0.742 ± 0.034 |
| FLG350 | 0.122 ± 0.026 | 0.181 ± 0.042 | 0.048 ± 0.001 | <LOQ | 0.227 ± 0.018 | 1.494 ± 0.093 | 0.024 ± 0.005 | 0.071 ± 0.012 | 0.733 ± 0.052 |
| FLG450 | 0.248 ± 0.044 | 0.254 ± 0.031 | 0.009 ± 0.001 | <LOQ | 0.262 ± 0.005 | 2.678 ± 0.027 | 1.107 ± 0.020 | 0.059 ± 0.005 | 0.547 ± 0.110 |

Table S 4. Dissolved organic carbon (DOC) and total dissolved nitrogen (TDN) concentrations from leached mineral and organic soil from the Nederland and Flagstaff sites. Mineral and organic soil were added at 0.5 and 2 g $L^{-1}$, respectively.

| Site | Heating Temp. (ºC) | Layer | DOC ($mg_C$/L) | TDN ($mg_N$/L) |
|---|---|---|---|---|
| Nederland | CTRL | Organic | 50.1±1.6 | 1.6±2.3 |
| | 150 | | 57.4±0.4 | 0.4±0.6 |
| | 250 | | 8.8±0.2 | 0.2±0.2 |
| | 350 | | 6.4±0 | 0±0.1 |
| | 450 | | 1±0 | 0±0.1 |
| | CTRL | Mineral | 3.1±1.7 | 1.7±0.3 |
| | 150 | | 8.6±3.4 | 3.4±0.6 |
| | 250 | | 16.7±4.6 | 4.6±2.3 |
| | 350 | | 5.5±0.9 | 0.9±1 |
| | 450 | | 0.4±0.1 | 0.1±0.1 |
| | 550 | | 0±0 | 0±0 |
| Flagstaff | CTRL | Organic | 70.4±0.9 | 0.9±1 |
| | 150 | | 64.3±0.9 | 0.9±0.7 |
| | 250 | | 7.3±0.1 | 0.1±0.2 |
| | 350 | | 3.1±0 | 0±0.1 |
| | 450 | | 1.2±0 | 0±1.2 |
| | CTRL | Mineral | 3.1±0.4 | 0.4±0.3 |
| | 150 | | 12.1±4.5 | 4.5±0.8 |
| | 250 | | 9.2±2.3 | 2.3±1.2 |
| | 350 | | 3.3±0.6 | 0.6±0.7 |
| | 450 | | 0.3±0.1 | 0.1±0.1 |
| | 550 | | 0±0 | 0±0 |

Table S 5. Statistical comparison of averaged optical properties for Nederland and Flagstaff sites' mineral and organic soils. Numbers in table represent p-values from a student's t-test (one tailed) comparing the control sample (soil heated at 100 ºC) to different soil heating temperatures.

| Soil heating temperature | $UV_{254}$ ($cm^{-1}$) | SUVA254 (L $mg_C^{-1}$ $m^{-1}$) | E2/E3 | S ($nm^{-1}$) |
|---|---|---|---|---|
| 100-150 | 0.041 | 0.089 | 0.279 | 0.484 |
| 100-250 | 0.014 | 0.010 | 0.137 | 0.123 |
| 100-350 | 0.027 | 0.020 | 0.014 | 0.442 |
| 100-450 | 0.007 | 0.024 | 0.145 | 0.308 |
| | $S_R$ | A (RU) | B (RU) | C (RU) |
| 100-150 | 0.267 | 0.345 | 0.362 | 0.013 |
| 100-250 | 0.144 | 0.041 | 0.119 | 0.039 |
| 100-350 | 0.106 | 0.051 | 0.112 | 0.050 |
| 100-450 | 0.296 | 0.361 | 0.114 | 0.470 |
| | T (RU) | FI | Peak Em 370 (nm) | SpA (RU L $mg_C^{-1}$) |
| 100-150 | 0.425 | 0.357 | 0.159 | 0.094 |
| 100-250 | 0.152 | 0.046 | 0.045 | 0.001 |
| 100-350 | 0.143 | 0.068 | 0.010 | 0.012 |
| 100-450 | 0.124 | 0.215 | 0.012 | 0.012 |
| | SpB (RU L $mg_C^{-1}$) | SpC (RU L $mg_C^{-1}$) | SpT (RU L $mg_C^{-1}$) | Phi_f |
| 100-150 | 0.417 | 0.137 | 0.468 | 0.045 |
| 100-250 | 0.208 | 0.001 | 0.457 | 0.013 |
| 100-350 | 0.263 | 0.010 | 0.056 | 0.027 |
| 100-450 | 0.185 | 0.012 | 0.080 | 0.007 |

Table S 6. Optical property data water extractable organic carbon from composite sample leachates. Optical property definitions are provided in Table S 2.

| Sample | $UV_{254}$ ($cm^{-1}$) | E2/E3 | S ($nm^{-1}$) | $S_R$ | A (RU) | B (RU) | C (RU) | T (RU) | FI | Peak Em 370 (nm) | $\Phi_f$ |
|---|---|---|---|---|---|---|---|---|---|---|---|
| DW1 | 0.115 | 4.97 | 0.0164 | 0.511 | 1.00 | 0.22 | 0.45 | 0.20 | 1.46 | 466 | 0.0116 |
| DW1225 | 0.164 | 6.40 | 0.0167 | 0.757 | 30.60 | 2.85 | 15.06 | 3.16 | 1.37 | 442 | 0.0466 |
| DW2 | 0.060 | 5.37 | 0.0171 | 0.396 | 0.55 | 0.29 | 0.27 | 0.23 | 1.56 | 466 | 0.0162 |
| DW2225 | 0.176 | 5.23 | 0.0152 | 0.752 | 23.40 | 2.91 | 12.06 | 2.61 | 1.21 | 462 | 0.0307 |
| DW3 | 0.137 | 5.24 | 0.0167 | 0.526 | 1.37 | 0.22 | 0.61 | 0.26 | 1.49 | 464 | 0.0126 |
| DW3225 | 0.178 | 6.68 | 0.0170 | 0.873 | 24.68 | 2.77 | 12.28 | 3.25 | 1.36 | 444 | 0.0354 |
| NYEA | 0.121 | 4.90 | 0.0158 | 0.565 | 1.09 | 0.22 | 0.50 | 0.32 | 1.45 | 466 | 0.0113 |
| NYEA225 | 0.168 | 6.41 | 0.0172 | 0.832 | 30.58 | 3.81 | 14.62 | 4.57 | 1.45 | 444 | 0.0445 |
| NYKEN | 0.177 | 4.40 | 0.0154 | 0.532 | 1.44 | 0.25 | 0.72 | 0.28 | 1.48 | 468 | 0.0097 |
| NYKEN225 | 0.151 | 4.89 | 0.0150 | 0.816 | 20.97 | 3.46 | 10.61 | 3.75 | 1.36 | 448 | 0.0321 |
| NYNN | 0.193 | 4.23 | 0.0145 | 0.625 | 1.77 | 0.27 | 0.86 | 0.36 | 1.45 | 468 | 0.0102 |
| NYNN225 | 0.171 | 6.33 | 0.0175 | 0.698 | 47.47 | 5.19 | 22.49 | 6.07 | 1.42 | 440 | 0.0587 |
| NYRR | 0.130 | 5.14 | 0.0165 | 0.501 | 1.37 | 0.19 | 0.63 | 0.26 | 1.48 | 464 | 0.0122 |
| NYRR225 | 0.212 | 7.58 | 0.0185 | 0.757 | 104.34 | 13.09 | 47.90 | 12.17 | 1.33 | 446 | 0.0718 |
| WM35 | 0.088 | 4.86 | 0.0161 | 0.371 | 0.76 | 0.50 | 0.38 | 0.31 | 1.54 | 462 | 0.0107 |
| WM35225 | 0.215 | 6.78 | 0.0173 | 0.699 | 57.74 | 4.87 | 26.80 | 5.31 | 1.27 | 442 | 0.0468 |
| WM40 | 0.085 | 4.84 | 0.0174 | 0.395 | 0.64 | 0.56 | 0.34 | 0.36 | 1.52 | 464 | 0.0088 |
| WM40225 | 0.125 | 4.50 | 0.0149 | 0.696 | 5.00 | 0.87 | 2.74 | 1.21 | 1.36 | 458 | 0.0186 |
| WM49 | 0.072 | 4.85 | 0.0163 | 0.495 | 0.63 | 0.16 | 0.30 | 0.15 | 1.46 | 466 | 0.0132 |
| WM49225 | 0.149 | 4.48 | 0.0146 | 0.511 | 17.59 | 3.25 | 9.06 | 2.74 | 1.32 | 456 | 0.0232 |

**Supplementary Figures**

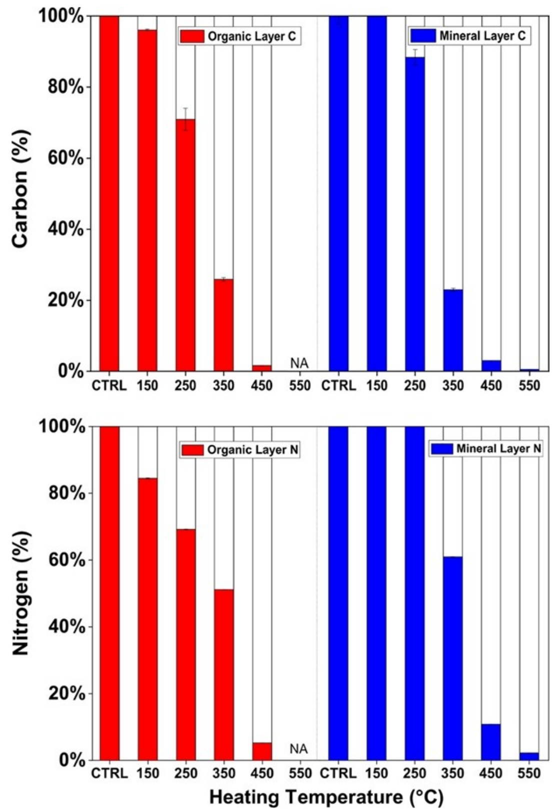


Figure S 1. Carbon (top panel) and nitrogen (bottom panel) remaining in organic and mineral soil horizons after heating from the NED site. CTRL = control. C and N % is the mass of C or N normalized to soil mass. Data from Hohner et al., 2019. [2]

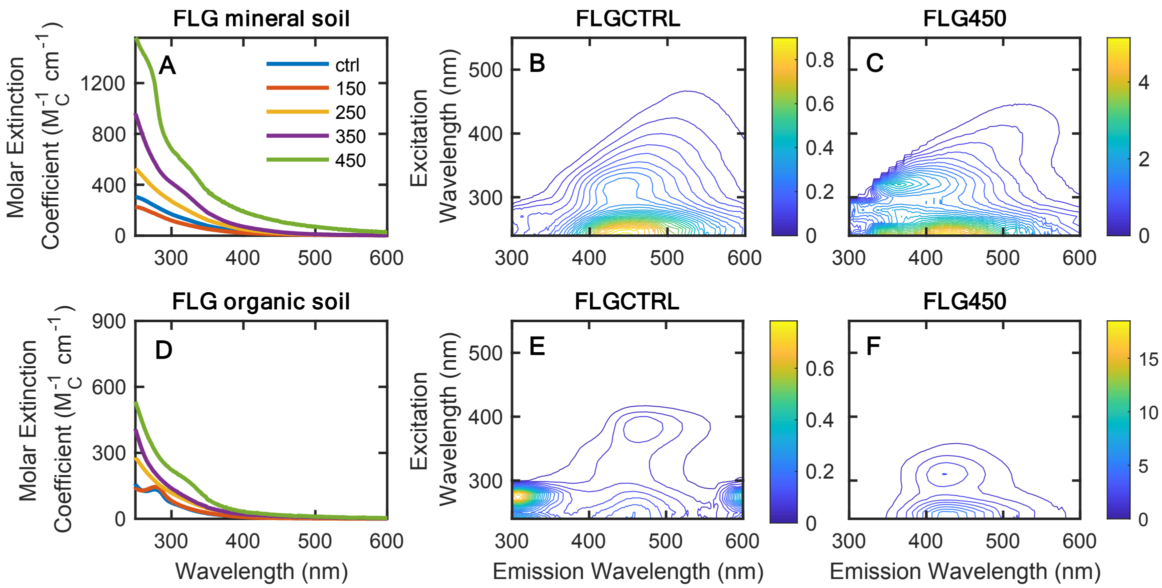


Figure S 2. Change in optical properties of water soluble organic carbon from mineral (top row) and organic soil (bottom row) from Flagstaff site. (A and D) Absorbance spectra normalized to carbon concentration. (B-C and E-F) Fluorescence spectra normalized to carbon concentration (units of RU L $mg_C^{-1}$).

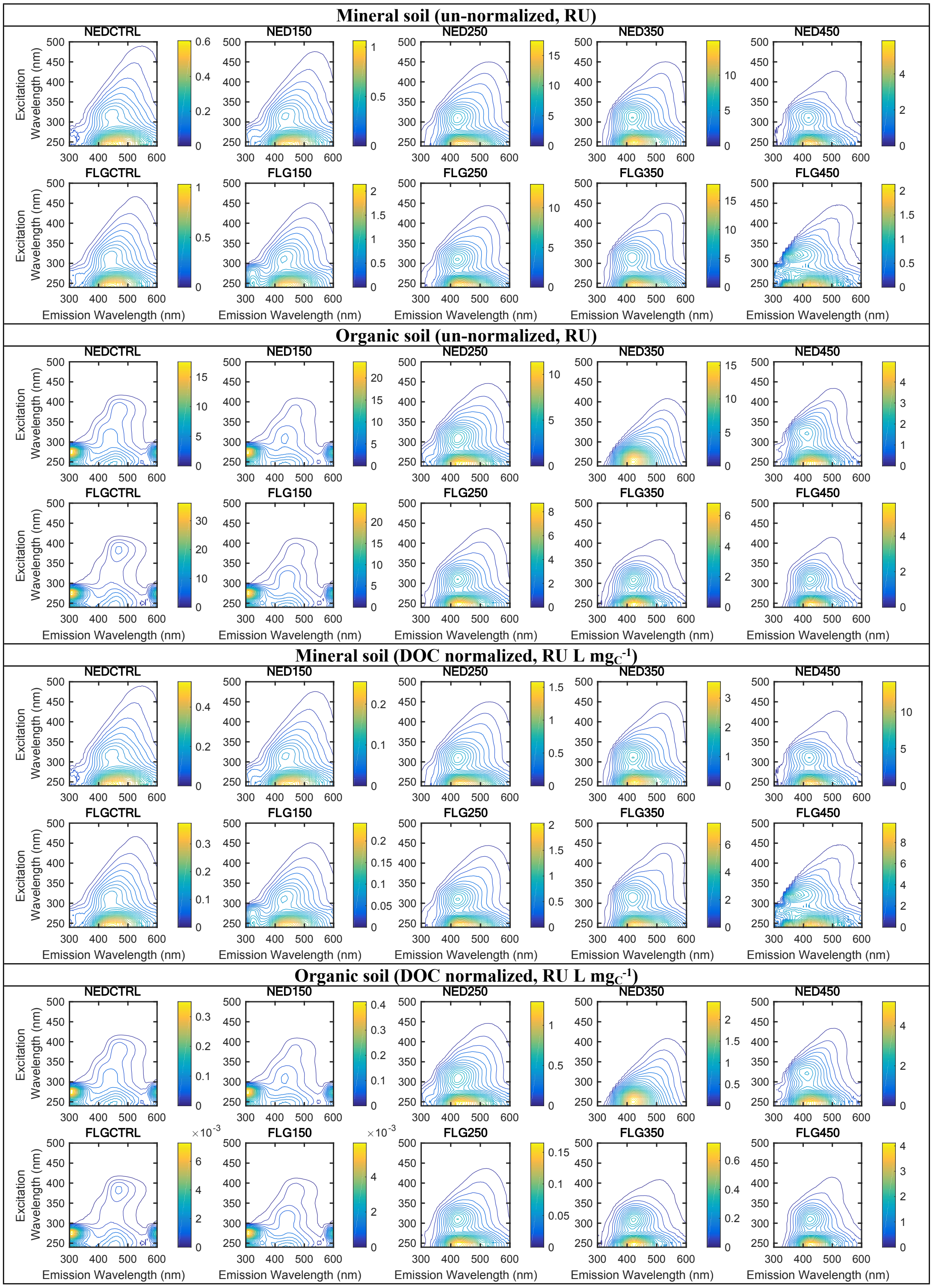


Figure S3. Fluorescence EEMs for mineral and organic soil leachates from NED and FLG sites. EEMs shown in Raman Units (RU) are corrected for sample dilution. Carbon-normalized EEMs were obtained by dividing by DOC concentration. The intensity at an excitation/emission pair of ~270nm/600nm in CTRL and 150 ºC heated organic soil is second order fluorescence as a result of the intense peak at ~270nm/300nm.

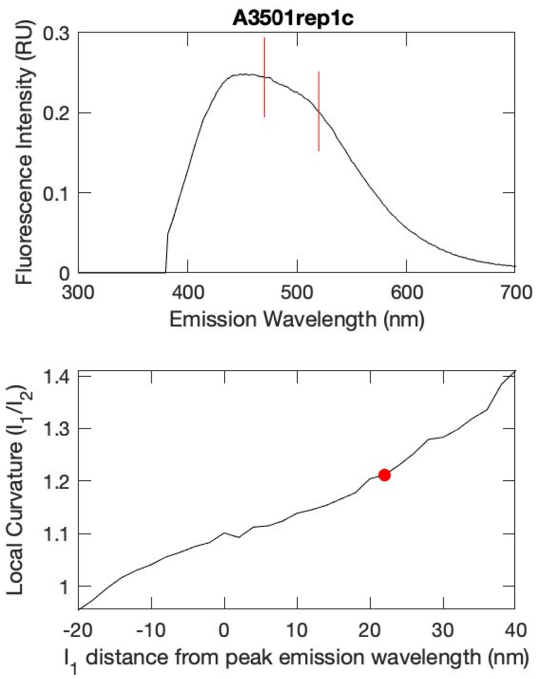


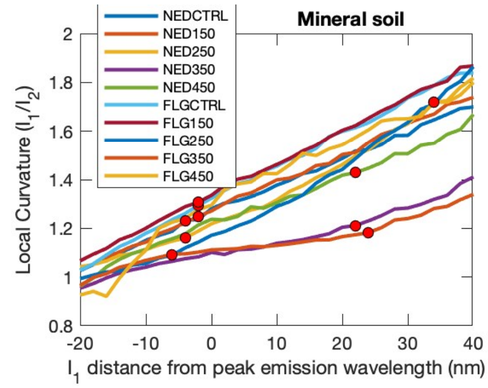


| Sample | Calculated FI | $I_1$ Distance from peak emission (nm) |
|---|---|---|
| NEDCTRL | 1.2325 | -4 |
| NED150 | 1.2497 | -2 |
| NED250 | 1.1598 | -4 |
| NED350 | 1.2115 | 22 |
| NED450 | 1.4286 | 22 |
| FLGCTRL | 1.2938 | -2 |
| FLG150 | 1.3071 | -2 |
| FLG250 | 1.0902 | -6 |
| FLG350 | 1.1823 | 24 |
| FLG450 | 1.7192 | 34 |

Figure S 4. (Left panel) Fluorescence emission spectrum at an excitation wavelength of 370 nm (top) and local curvature (bottom) as a function of location relative to the peak emission. Local curvature is the ratio of two intensities ($I_1/I_2$) spaced 50 nm apart where $I_1$ is the shorter wavelength. The marker indicates where FI is calculated based on the prescribed emission wavelengths of 420 and 470 nm (red, vertical lines). (Right panel) Fluorescence index (FI) calculated based on prescribed emission wavelengths and distance of peak emission maximum from 420 nm. Samples shown are for mineral soil.

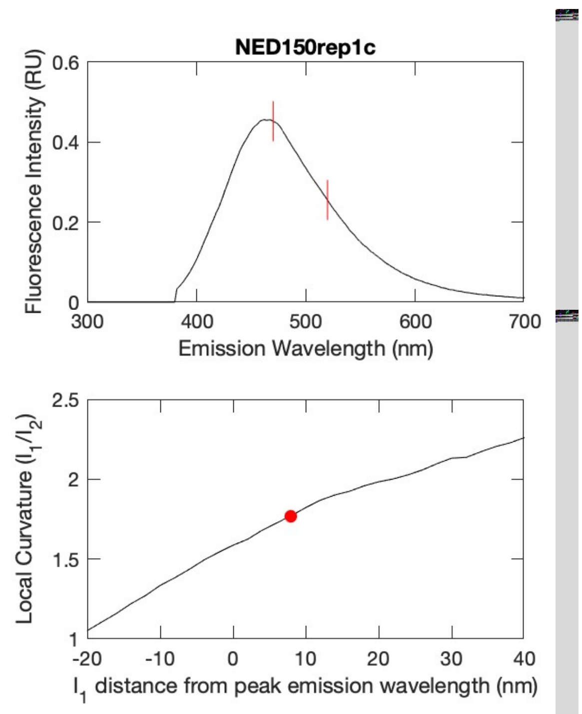


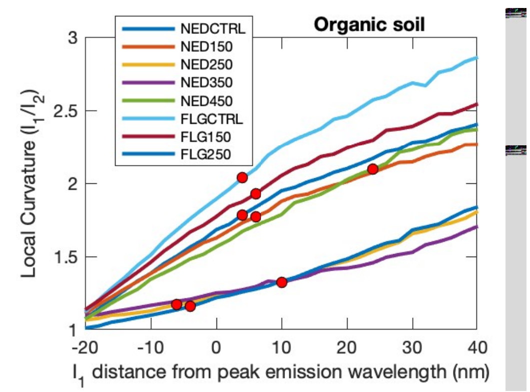


| Sample | Calculated FI | $I_1$ Distance from peak emission (nm) |
|---|---|---|
| NEDCTRL | 1.7842 | 4 |
| NED150 | 1.7692 | 6 |
| NED250 | 1.1703 | -6 |
| NED350 | 1.3218 | 10 |
| NED450 | 2.0956 | 24 |
| FLGCTRL | 2.0351 | 4 |
| FLG150 | 1.9259 | 6 |
| FLG250 | 1.1588 | -4 |

Figure S 5. (Left panel) Fluorescence emission spectrum at an excitation wavelength of 370 nm (top) and local curvature (bottom) as a function of location relative to the peak emission. Local curvature is the ratio of two intensities ($I_1/I_2$) spaced 50 nm apart where $I_1$ is the shorter wavelength. The marker indicates where FI is calculated based on the prescribed emission wavelengths of 420 and 470 nm (red, vertical lines). (Right panel) Fluorescence index (FI) calculated based on prescribed emission wavelengths and distance of peak emission maximum from 420 nm. Samples shown are for organic soil.

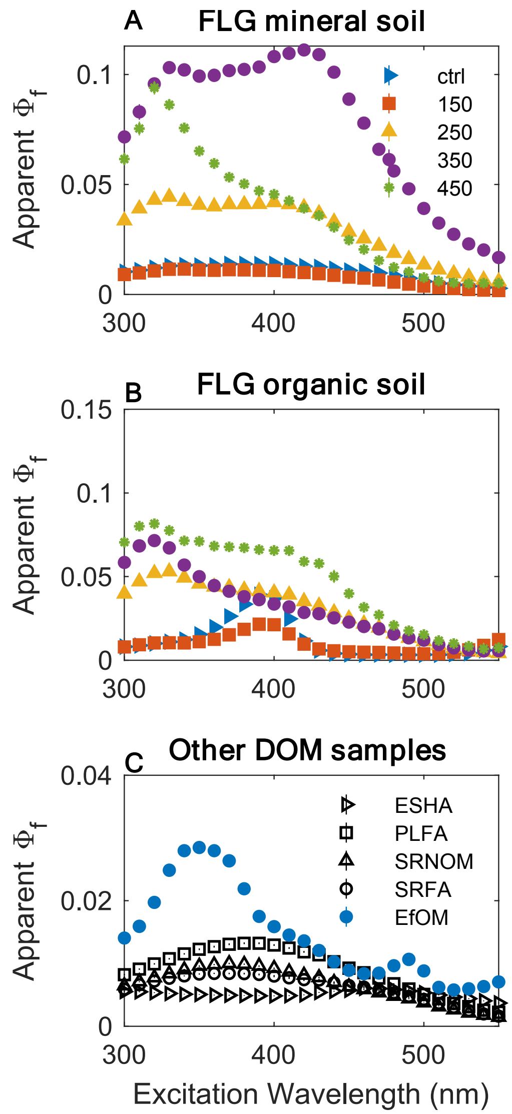


Figure S 6. Apparent fluorescence quantum yields ($\Phi_f$) for (A) Flagstaff mineral soil leachates, (B) Flagstaff organic soil leachates, and (C) select DOM samples. For 3a and 3b, colors represent different soil heating temperatures (in ºC). For Figure 3c, different symbols represent various organic matter types: ESHA (Elliot Soil humic acid I), PLFA (Pony Lake fulvic acid), Suwannee River Natural Organic Matter (SRNOM II), Suwannee River fulvic acid (SRFA I), and EfOM (effluent organic matter). Error bars represent the standard deviation from duplicate measurements. If not visible, then the error bars are smaller than the symbols.

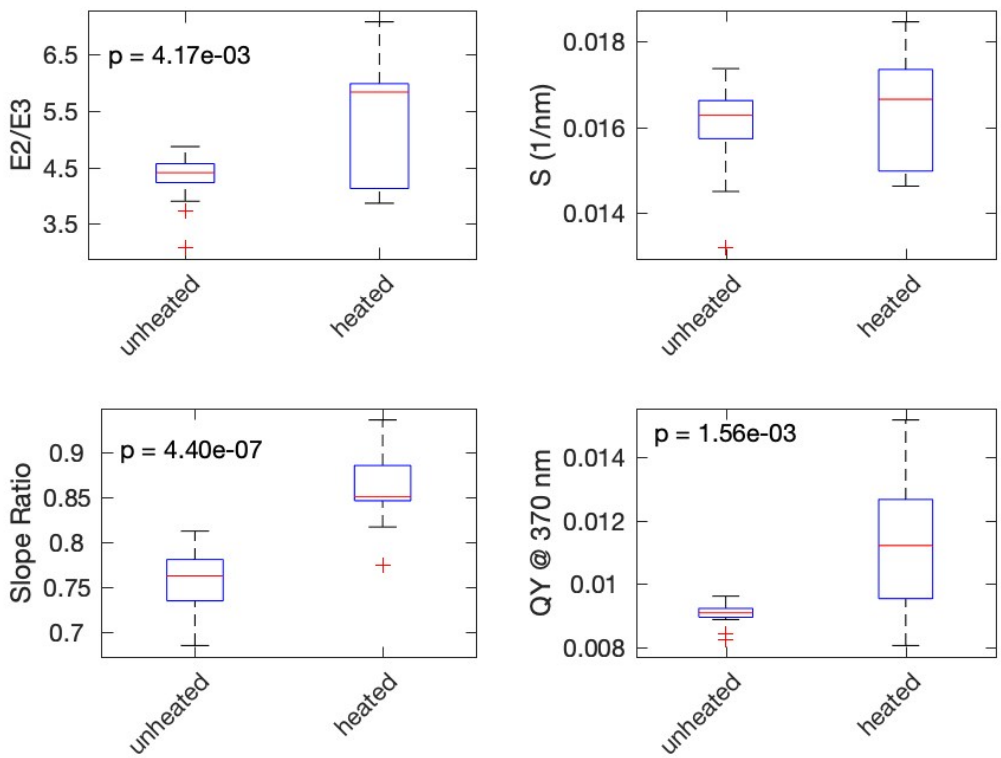


Figure S 7. Box plot of optical properties water extractable organic carbon from composite sample leachates (DW, NY, WM; see Table S1). All unheated and heated properties were averaged.

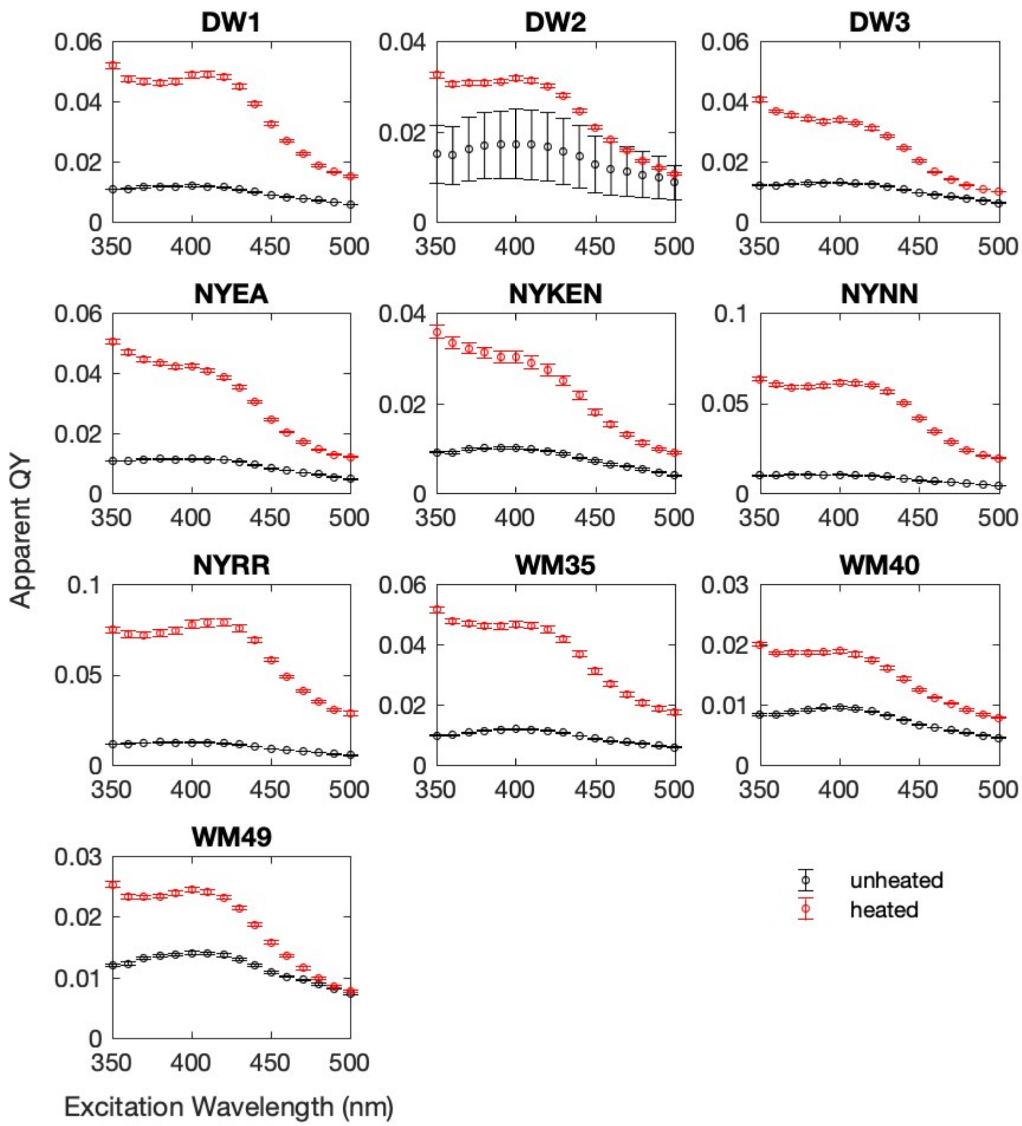


Figure S 8. Apparent fluorescence quantum yield as a function of excitation wavelength for water extractable organic carbon from composite sample leachates.

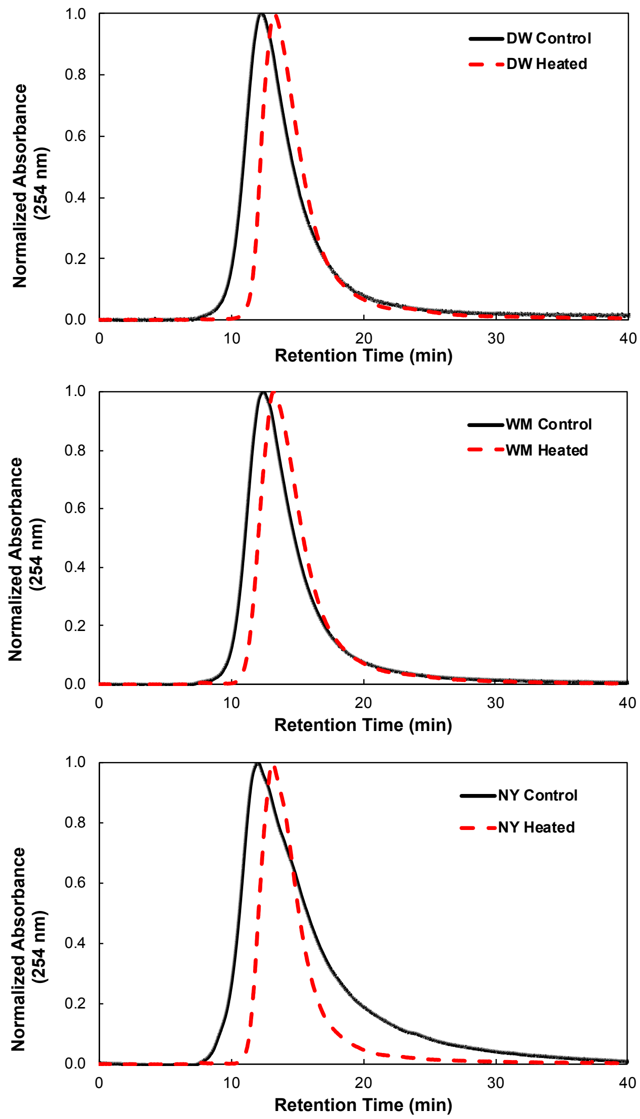


Figure S 9. Size exclusion chromatograms (SEC) for unheated (black, solid line) and 250 ºC heated (red, dashed line) soil leachates. DW = Denver Water; WM = Westminster; NY = New York. Samples identities and descriptions are provided in ESI Table S1. Data are from Hohner et al.[3]

## Supplementary Text

### Text S 1. Muffle furnace justification

There has been recent interest in understanding the impact of wildfires on water quality, including how it impacts the physicochemical properties of the mobilized DOC after a fire. For example, studies by others have shown an increase in DOC after a wildfire, coupled also with fluctuations in other chemical measures such as formation of disinfection byproducts (DBP). [4] Collecting and analyzing ash and soil samples from naturally burned watersheds is a useful way of understanding how wildfires effect landscapes and riverine environments. [5-7] Ash consists of charred organic material from the O-horizon that can be collected by designating two visual specifications; black ash (moderate burning) and white ash (severe burning). [4] Soil samples are collected from the A-horizon and consist of a mix of mineral and organic constituents. Specifically, both ash and soil have notable effects on water quality in burned watersheds. Because of the long-lasting ramifications wildfires have on aquatic systems, [8] monitoring surface waters is highly useful to researchers and water providers alike.

Due to the lack of true pre-rainstorm burn sites, the collection of ash and soil from burned watersheds tends to be a challenging task. Wildfires weaken hill slope stability and create water repellant layers within soil, thus creating swells of stormwater erosion directly after burn events. Therefore, there is typically a narrow timespan for sample collection before much of the ash and topsoil is lost to proximal surface waters in the form of dissolved compounds and suspended solids. [9]

Moreover, solely studying environmental samples lacks the degrees of control necessary for understanding more fundamental concepts. Depending on the goal of a given study, controlling factors like temperature, burn time, and oxygen availability can be highly useful. Prescribed burns and simulated burning techniques in laboratories are popular alternatives because of their ability to control some of these factors. Additionally, thermally treated ash and soil produced from these alternatives can be used to create surrogate water quality samples by leaching natural organic matter into laboratory grade water until post-wildfire stream conditions are matched.

Prescribed burns have been proven to be a highly effective alternative because of their strong likeness to natural wildfires. [4] However, prescribed burns can be limited to lower burn temperatures due to the challenges associated with controlling high intensity wildfires. For this reason, bench scale approaches are a more popular option because of the high degree of control on burn temperature and duration; but questions arise around these methods' likeness to natural and prescribed burns. For example, Santin et al. found that soil organic matter (SOM) required higher temperatures (600-700 °C) to transform into more aromatic forms during prescribed burning rather than what was previously reported (300-500 °C) from bench scale experiments. [10]

In order to further understand the observed effects of wildfires on the physicochemical properties of DOC, proper control experiments need to be developed. Further research is needed to improve and standardize simulated burn techniques; nevertheless, a variety of methods have already been put into use in other publications. A conventional bench scale setup involves heating field samples in a muffle furnace, [11] however other studies have opted for heating in open pans[12] with heat sources such as heat guns. [13] Heat durations are widely variable, with times as low as thirty minutes[14] and as high as two hours. [11] Different temperature ramp protocols for muffle furnaces have been developed to asses aggregate structure, [14] or to prevent sudden soil ignition. [15] Techniques also exist for homogenizing soils during heating, such as turning samples over every 5 minutes while being treated in a muffle furnace. [16] The large variety of methods available to researchers provides ample options, however it also makes comparing results difficult from study to study. [17]

In our work, we have used the method employing a muffle furnace, with samples homogenized and exposed to a certain temperature setting for 2-hours. This method has allowed us (and others) to provide concrete mechanistic information regarding the transformations of the soil organic matter, and ultimately how those impact the DOC exported.

**Text S 2. Fluorescence Index**

We evaluated the appropriateness of the fluorescence index (FI) as a metric for describing water extractable organic matter (WEOM) from laboratory heated soil. FI is defined as the ratio of fluorescence intensities – specifically, 470 nm to 520 nm – at an excitation wavelength of 370 nm. FI has been linked to aquatic dissolved organic matter (DOM) source and structure, namely its molecular weight and aromaticity. Recent work has called into question whether FI accurately captures the local curvature for the diverse array of DOM samples to which it has been applied. [18] We applied the analysis described by Korak et al. [18] to these samples as described below.

Briefly, the local curvature is the ratio of fluorescence intensities at two emission wavelengths ($I_1$ and $I_2$), where $I_1$ is at the maximum emission wavelength and $I_2$ is the intensity at 50 nm past $I_1$. ESI Figures S3 and S4 show the results of this analysis for NED and FLG soil leachates. FI was a good approximation of local curvature for CTRL, 150 ºC, and 250 ºC heated soil leachates, with peak emission maxima having distances from $I_1$ of less than 10 nm. For both mineral and organic soil, there was actually a decrease in FI between the CTRL and 250 ºC heated samples. Calculated FI was indeed higher for 450 ºC heated soil leachates compared to CTRL samples, consistent with previous reports. [4,19,20] However, FI is no longer a reasonable approximation of local curvature for 350 ºC and 450 ºC heated samples, with peak distances from $I_1$ ranging from 22 nm to 34 nm (SI Figures S4 and S5).

**References**


(1) McKay, G.; Korak, J. A.; Erickson, P. R.; Latch, D. E.; McNeill, K.; Rosario-Ortiz, F. L. The Case Against Charge Transfer Interactions in Dissolved Organic Matter Photophysics. *Environmental Science & Technology* **2018**, *52* (2), 406–414.

(2) Hohner, A. K.; Rhoades, C. C.; Wilkerson, P.; Rosario-Ortiz, F. L. Wildfires Alter Forest Watersheds and Threaten Drinking Water Quality. *Accounts of Chemical Research* **2019**, *52* (5), 1234–1244.

(3) Hohner, A. K.; Summers, R. S.; Rosario-Ortiz, F. L. Laboratory Simulation of Postfire Effects on Conventional Drinking Water Treatment and Disinfection Byproduct Formation. *AWWA Water Science* **2019**, e1115.

(4) Wang, J.-J.; Dahlgren, R. A.; Chow, A. T. Controlled Burning of Forest Detritus Altering Spectroscopic Characteristics and Chlorine Reactivity of Dissolved Organic Matter: Effects of Temperature and Oxygen Availability. *Environmental Science & Technology* **2015**, *49* (24), 14019–14027.
(5) Hohner, A. K.; Cawley, K.; Oropeza, J.; Summers, R. S.; Rosario-Ortiz, F. L. Drinking water treatment response following a Colorado wildfire. *Water Research* **2016**, *105* (C), 187–198.
(6) Knicker, H.; Almendros, G.; Gonzalez-Vila, F. J.; Gonzalez-Perez, J. A.; Polvillo, O. Characteristic alterations of quantity and quality of soil organic matter caused by forest fires in continental Mediterranean ecosystems: a solid-state 13C NMR study. *Eur J Soil Science* **2006**, *57* (4), 558–569.
(7) Larsen, I. J.; MacDonald, L. H.; Brown, E.; Rough, D.; Welsh, M. J.; Pietraszek, J. H.; Libohova, Z.; de Dios Benavides-Solorio, J.; Schaffrath, K. Causes of Post-Fire Runoff and Erosion: Water Repellency, Cover, or Soil Sealing? *Soil Science Society of America Journal* **2009**, *73* (4), 1393.
(8) Rhoades, C. C.; Entwistle, D.; Butler, D. The influence of wildfire extent and severity on streamwater chemistry, sediment and temperature following the Hayman Fire, Colorado. *International Journal of Wildland Fire* **2011**, *20* (3), 430.
(9) Smith, H. G.; Sheridan, G. J.; Lane, P. N. J.; Nyman, P.; Haydon, S. Wildfire effects on water quality in forest catchments: A review with implications for water supply. *Journal of Hydrology* **2011**, *396* (1-2), 170–192.
(10) Forest floor chemical transformations in a boreal forest fire and their correlations with temperature and heating duration. *Geoderma* **2016**, *264*, 71–80.
(11) Cawley, K. M.; Hohner, A. K.; Podgorski, D. C.; Cooper, W. T.; Korak, J. A.; Rosario-Ortiz, F. L. Molecular and Spectroscopic Characterization of Water Extractable Organic Matter from Thermally Altered Soils Reveal Insight into Disinfection Byproduct Precursors. *Environmental Science & Technology* **2017**, *51* (2), 771–779.
(12) Hogue, B. A.; Inglett, P. W. Nutrient release from combustion residues of two contrasting herbaceous vegetation types. *Science of The Total Environment* **2012**, *431*, 9–19.
(13) Wieting, C.; Ebel, B. A.; Singha, K. Quantifying the effects of wildfire on changes in soil properties by surface burning of soils from the Boulder Creek Critical Zone Observatory. *Journal of Hydrology: Regional Studies* **2017**, *13*, 43–57.
(14) Jian, M.; Berli, M.; Ghezzehei, T. A. Soil Structural Degradation During Low-Severity Burns. *Geophys. Res. Lett.* **2018**, *45* (11), 5553–5561.
(15) Fernández, I.; Cabaneiro, A.; Carballas, T. Organic matter changes immediately after a wildfire in an atlantic forest soil and comparison with laboratory soil heating. *Soil Biology and Biochemistry* **1997**, *29* (1), 1–11.
(16) Bodí, M. B.; Mataix-Solera, J.; Doerr, S. H.; Cerdà, A. The wettability of ash from burned vegetation and its relationship to Mediterranean plant species type, burn severity and total organic carbon content. *Geoderma* **2011**, *160* (3), 599–607.

(17) Bodí, M. B.; Martin, D. A.; Balfour, V. N.; Santín, C.; Doerr, S. H.; Pereira, P.; Cerdà, A.; Mataix-Solera, J. Wildland fire ash: Production, composition and eco-hydro-geomorphic effects. *Earth Science Reviews* **2014**, *130*, 103–127.
(18) Korak, J. A.; Dotson, A. D.; Summers, R. S.; Rosario-Ortiz, F. L. Critical analysis of commonly used fluorescence metrics to characterize dissolved organic matter. *Water Research* **2014**, *49*, 327–338.
(19) Wang, J.-J.; Dahlgren, R. A.; Erşan, M. S.; Karanfil, T.; Chow, A. T. Wildfire Altering Terrestrial Precursors of Disinfection Byproducts in Forest Detritus. *Environmental Science & Technology* **2015**, *49* (10), 5921–5929.
(20) Cawley, K. M.; Hohner, A. K.; McKee, G. A.; Borch, T.; Omur-Ozbek, P.; Oropeza, J.; Rosario-Ortiz, F. L. Characterization and spatial distribution of particulate and soluble carbon and nitrogen from wildfire-impacted sediments. *J Soils Sediments* **2018**, 1–13.